STUDIES OF A SLOTTED IRIS STRUCTURE (DISPERSION CURVE, COUPLING, FLATNESS, AND ELECTRON ANALOG EXPERIMENT)

H. Eschelbacher, M. Kuntze, D. Schinzel, J. Vetter
Institut für Experimentelle Kernphysik
der Universität und des Kernforschungszentrums Karlsruhe

Bi-periodic structure

To enable the full utilization of the advantages of an AP-structure for a superconducting linear accelerator, detailed studies on a bi-periodic slotted-iris-structure have been performed, the main goal beeing to arrive at simultaneously high shuntimpedance and high group velocity for a structure that can be plated with a superconducting layer. A demountable 8-cell-model (fig. 1) has been used [1]. From the measurements of the field distributions the dependence of the flatness on the stop band width has been derived. The results indicate a direct proportionality between flatness and stop band width.

For the interpretation of the experimental results it was necessary to take into account not only the direct coupling between adjacent cells but also the coupling between alternate cells (skip coupling). A dispersion relation has been derived from field expansion using waveguide modes [2]. The same dispersion relation can also be deduced from a mechanical model of coupled pendula [1]. For the case of unequal zero mode resonances ($\omega_{01} \neq \omega_{02}$), which is obtained by detuning one of the two kinds of cells, the dispersion relation is given by

$$2\,\frac{\omega_o^2-\omega_n^2}{\omega_n^2} = k_1'+k_2+k_3+k_4-(k_3+k_4)\cos 2\phi_n \mp \sqrt{(k_1'-k_2+k_3-k_4-(k_3-k_4)\cos 2\phi_n)^2+4k_1k_2\cos^2\phi_n}$$

where $k_1' = k_1 - \frac{\omega_{01}^2-\omega_o^2}{\omega_o^2} = k_1 + \Delta$ if $\omega_{02} = \omega_o$. The constant k_1 is a measure for the coupling in the unperturbed case ($\omega_{01} = \omega_{02}$). Insertion of the measured frequencies into the dispersion relation yields the coupling coefficients. Fig. 2 gives an example for the dispersion curve.

Furthermore the dependence of the coupling coefficients on the cell lengths has been studied. The following proportionalities hold

$$1/k_1 \sim 1 + L_B/L_i$$

$$1/k_2 \sim 1 + L_k/L_i$$

$$k_3 \sim \frac{L_i}{L_B}\exp(-\text{const. } L_k)$$

where L_i is a characteristic length of the coupling region. The variation of k_1 with L_B for various L_k (fig. 3) and for k_2 with L_k for various L_B (fig. 4) has been measured. k_3 was measured as a function of L_k for various L_B (fig. 5) and k_4 was found to be nearly zero. The experimental results are in good agreement with the theory [3].

Cylindrical drift tubes of length l were inserted into the accelerating cells in order to reduce the width of the stop band. The drift tube length has been varied and dispersion curve and field distribution were measured for each l (fig. 2). The condition for the elimination of the stop band is $k_2 = k_1'+2k_3$. The sum $k_1'+2k_3-k_2$ is plotted in fig. 6 versus drift tube length. That drift tube length, where the stop band is narrowest is indicated by the minimum. The square of the flatness is shown in the same figure. Obviously both functions have a common minimum.

Electron Analog experiment

An electron analog experiment allows to study the most essential features (e.g. beam loading) for a superconducting proton linear accelerator. Currents, voltages and rf-fields are reduced by the electron-proton mass ratio and the required rf-power by the square of this ratio. On the other hand all dynamical problems remain essentially unchanged

with electron of corresponding energies, i.e. the same velocity as for protons.

A first analog experiment had been carried out by the Los Alamos group at room temperature [4]. It is planned to perform a similar experiment at Karlsruhe with a superconducting structure. A description of the experimental arrangement and more detailed calculations are given by Vetter [5].

The present investigations are restricted to measurements at room temperature. In the near future measurements with a lead plated structure will be performed at He-temperature. It was decided to build a 1 m accelerator model for v/c = 0.5. This value corresponds to a kinetic energy of 145 MeV for protons and 79 keV for electrons. All relevant parameters are listed in table 1. With the reasonable value of 10^5 for the improvement factor a power of only 7 µW/m is required for the energy gain of 3.8 keV/m.

On the other hand even with the very low beam current (55 nA) and the small rf-power requirements heavy beam loading is obtained in a superconducting structure with electrons. A beam loading factor of b = 30 at 1.8°K should be possible. The analog experiment with electrons will, therefore, be a powerful tool to study the problems of a superconducting linear accelerator with beam loading effects included.

A tiny focused electron beam is delivered from an electron gun (fig. 7). The beam is spread out by a chopper resonator which is exited in the TM_{110}-mode at the same frequency as the accelerator model. The resonator produces a deflecting magnetic field on the beam axis. The beam travels along a driftlength and is cut by an aperture into the electron bunches. With an rf-power of 200 W and the existing geometry the attainable bunch width is about 5° in phase. The relative phase of chopper and accelerator model is adjustable. The accelerator model consists of a 12-cell slotted iris structure with drift tubes. The rf-power is fed into the centre cell by means of a coupling loop critically coupled to the transmission line. The structure is operated in the π-mode at 760 MHz. After traversing the accelerator model the beam arrives at the energy analyser which is an intermediate image filter lens. There the particles are decelerated by the same high voltage as is applied to the electron gun. Therefore variations of the high voltage with respect to the energy measurement are eliminated. An additional and adjustable voltage compensates for the energy gain of the particles. Based on the work of Simpson [6] and Soa [7] the lens was redesigned and a detailed description is given by Vetter [5]. A precision of better than 1 % is obtained for the measurements of the energy gain. The beam finally hits a Faraday cup which is connected to a sensitive electrometer.

The entire beam path is about 4 m long. Several apertures, focussing coils and adjusting magnets are used for beam guidance. The earth's magnetic field has been nearly removed by µ-metal screening.

The accelerator model was tuned by geometrical variations of the various cells (e.g. adjusting the lengths of the drift tubes). The result of this procedure was an amplitude flatness of about 5 %. The field distribution in the 12-cell structure has been measured by the perturbation method [8]. From this measured field distribution the maximum energy gain has been calculated as a function of the initial energy W_o, the initial phase ϕ_o and the power dissipation P_s in the structure. The variation of v/c during acceleration has been taken into account. A value of (20,4 ± 0,6) M Ω/m for the shuntimpedance of the structure was the result of these calculations, according to a measured unloaded Q-value of 9900 ± 300 [9].

This value of the shuntimpedance which has been deduced from a measurement of the field distribution can be compared with the result derived from the energy gain of the electron beam. First the maximum energy gain of the unchopped beam was measured. Secondly chopped beam measurements have been performed for the energy gain as function of W_o and P_s for the optimum entry phase. Fig. 8 gives the cut-off curves of the energy analyser, taken with the chopped beam with different exitation powers. From both measurements, with the continuous and the chopped beam, the shuntimpedance of the structure was derived. The experimental determined energy gain as function of P_s as plotted in fig. 9 shows the expected straight line, with a slope which is just the square root of the shuntimpedance of the structure. The result of the electron beam measurements is Z = (19.8±0.4) MΩ/m. The excellent agreement with the computed results based on the perturbation measurements proves the satisfactory operation of the experimental set-up. Similar measurements with a superconducting structure are under preparation.

References

1) D. Schinzel
1968, External report 3/68-4, Kernforschungszentrum Karlsruhe

2) T. Nishikawa, S. Giordano, D. Carter
1966, Rev.Sci.Instr. 37, 652

3) H. Schopper
this conference, p.755

4) J.E. Brolley, C.R. Emigh, D.W. Mueller
1965, IEEE Trans.Nucl.Sci. NS-12, 144

5) J. Vetter
1968, Dissertation Karlsruhe

6) J.A. Simpson
1961, Rev.Sci.Instr. 32, 1283

7) E.A. Soa
Jenaer Jahrbuch 1, 115 (Carl Zeiss, Jena 1959)

8) L.C. Maier, J.C. Slater
1952, Journ. Appl. Phys. 23, 78

9) W. Jüngst, R. Hashmi, M. Kuntze, J. Vetter
1967, External report 3/67-15, Kernforschungszentrum Karlsruhe

Table 1:

Parameter for the superconducting electron analog experiment

	protons	electrons
v/c	0.5	
frequency	760 MHz	
cavity length	1 m	
current I_b	100µA	55 nA
kin. energy E_K	145 MeV	79 keV
energy gain ΔW	7 MeV/m	3.8 keV/m
beam power P_b	0.7 kW/m	0.21 mW/m
quality factor Q_o	10^9	10^9
shuntimpedance	$2 \cdot 10^6$ MΩ/m	$2 \cdot 10^6$ MΩ/m
power dissipation P_s	24,5 W/m	7,2 W/m
$b = P_b/P_s$	29	29

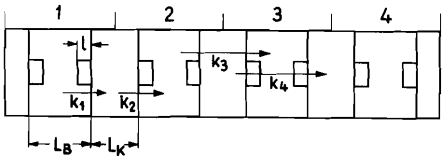

Fig. 1: Schematic diagram of the 4-cell AP-structure and definition of the coupling coefficients

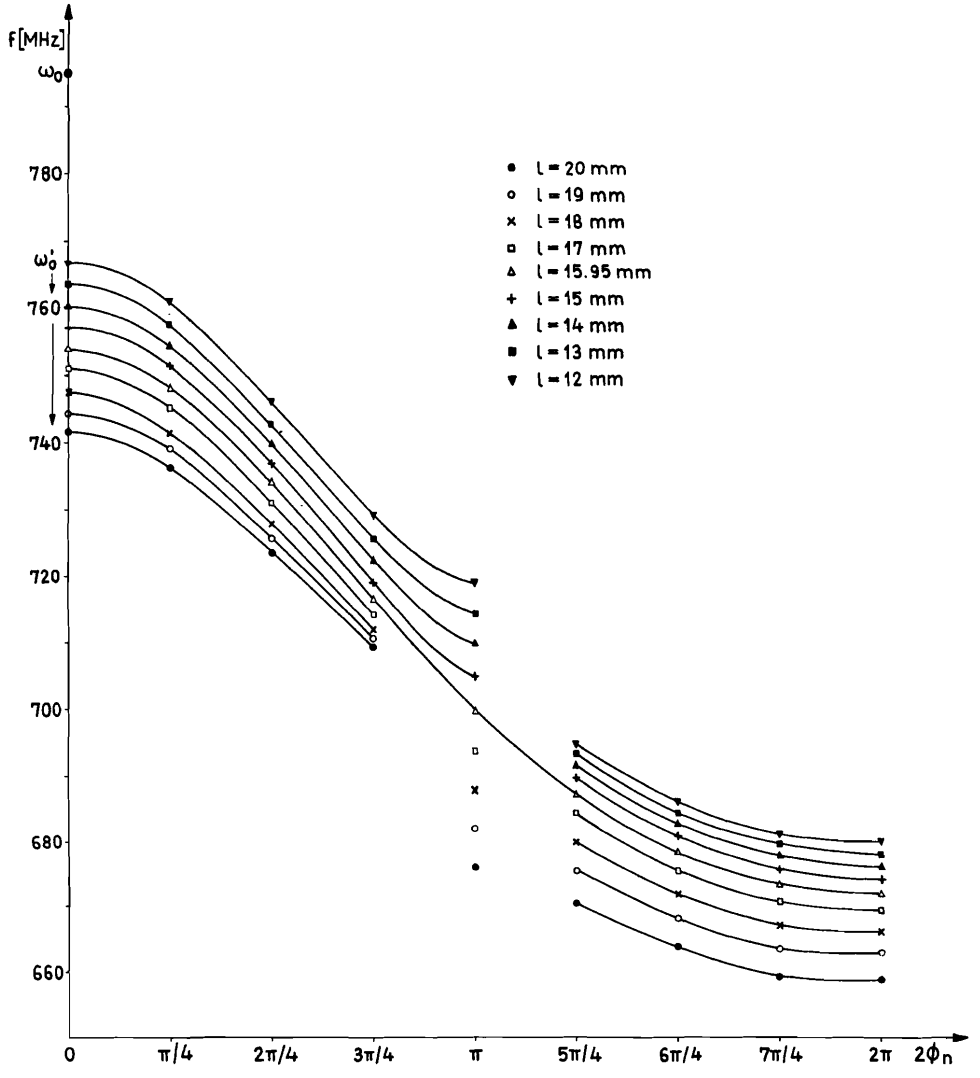

Fig. 2: Dispersion curves of an APS with drift tube length as parameter

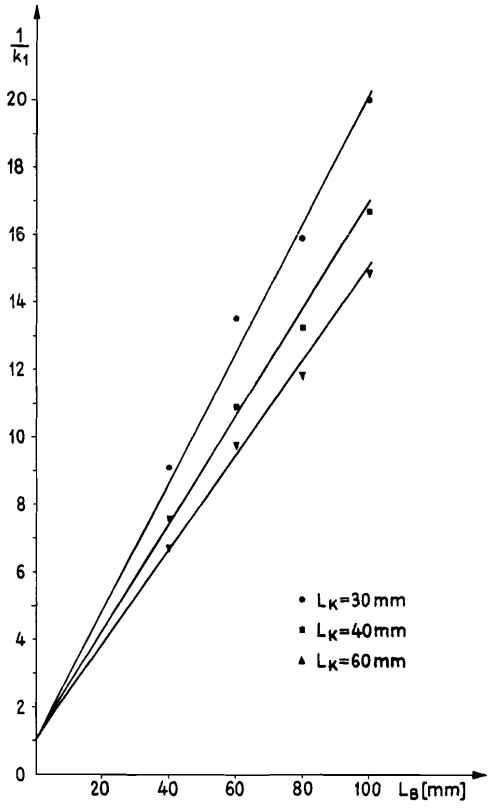

Fig. 3: Variation of k_1 with L_B for various L_K

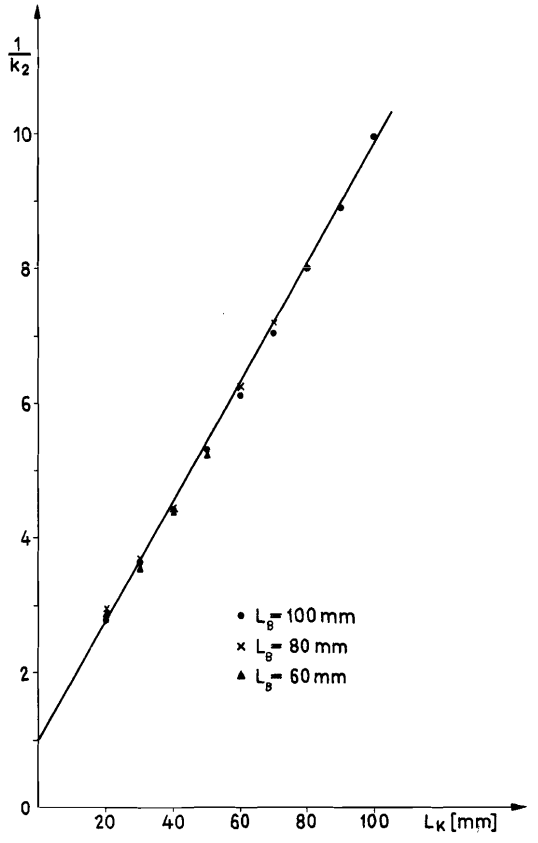

Fig. 4: Variation of k_2 with L_K for various L_B

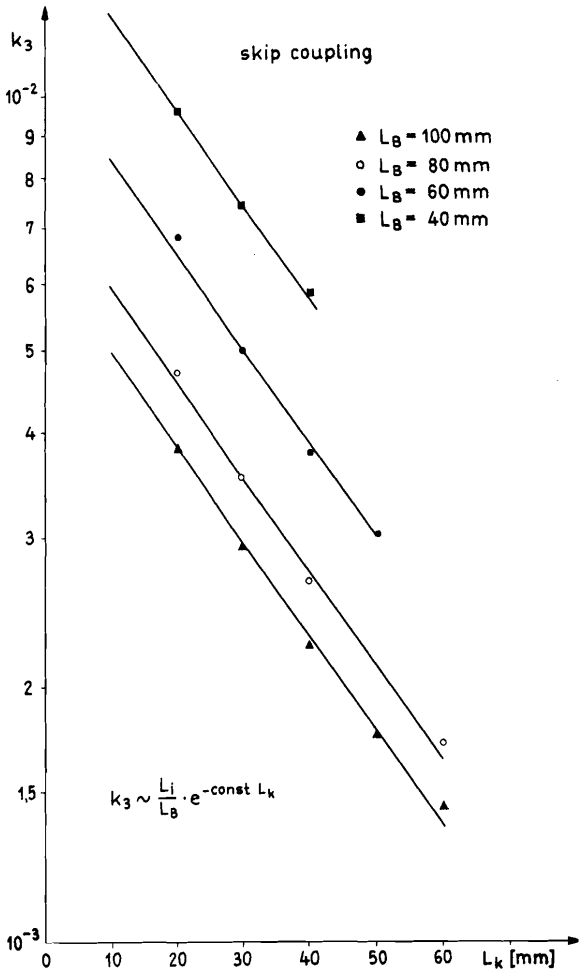

Fig. 5: k_3 as function of L_K for various L_B

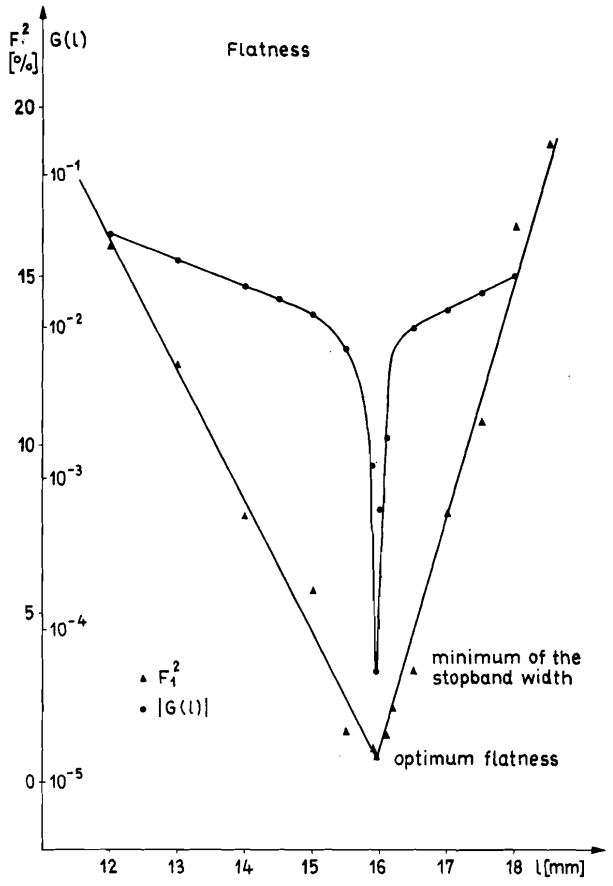

Fig. 6: Flatness F^2 as function of the reduction of the stopband width. $G(l) = k_1'+2k_3-k_2$ versus drift tube length. Both functions show a common minimum.

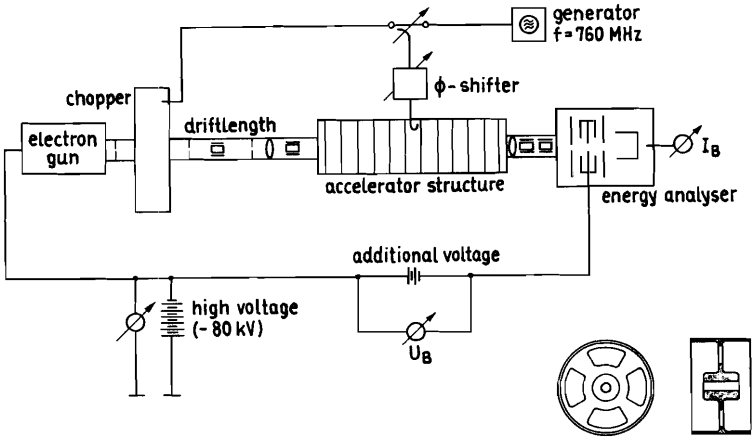

Fig. 7: Schematic outline of the electron analog experiment

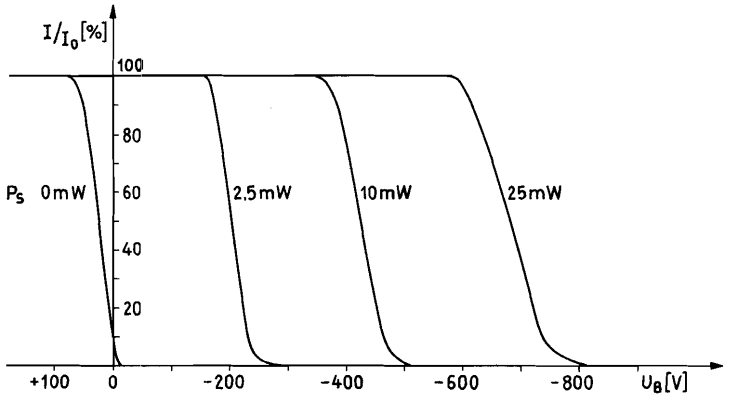

Fig. 8: Experimentaly determined cut-off curves of the energy analyser for the chopped beam taken with different excitation power into the accelerating structure. From the different shifts with respect to the OmW-curve the energy gain ΔW has been obtained.

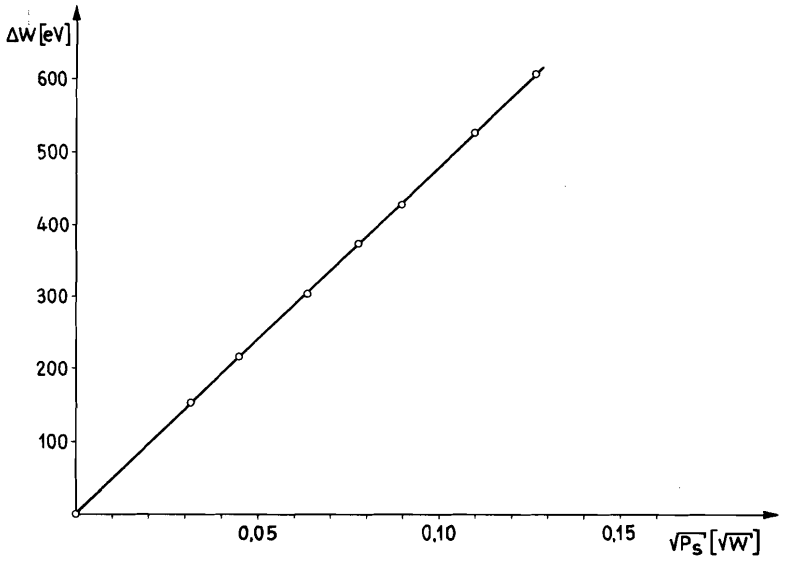

Fig. 9: The experimentaly determined energy gain as function of $\sqrt{P_s}$. The solid line is obtained from a least square fit.